Sensitivity Improvement of Infrared Imaging Video Bolometer for Divertor Plasma Measurement

K. Mukai,[1,2,a)] B. J. Peterson,[1,2] N. Ezumi,[3] N. Shigematsu,[3] S. Ohshima,[4] A. Miyashita,[5] and R. Matoike[5]

[1]*National Institute for Fusion Science, National Institutes of Natural Science, Toki, Gifu 509-5292, Japan*
[2]*SOKENDAI (The Graduate University for Advanced Studies), Toki, Gifu 509-5292, Japan*
[3]*Plasma Research Center, University of Tsukuba, Tsukuba, Ibaraki 305-8577 Japan*
[4]*Institute of Advanced Energy, Kyoto University, Uji, Kyoto 611-0011 Japan*
[5]*Graduated School of Energy Science, Kyoto University, Uji, Kyoto 611-0011 Japan*

(Presented XXXXX; received XXXXX; accepted XXXXX; published online XXXXX)
(Dates appearing here are provided by the Editorial Office)

Sensitivity of the infrared imaging video bolometer was improved for measurement of relatively low energy plasma radiation from the viewpoint of the metal foil absorber material. Photon energy of the radiation was considered up to 1 keV for divertor plasma measurement. The thickness of the foil absorber was evaluated not only for conventional heavy elements, e.g., platinum, but also for light elements by the relation between photon energy and attenuation length and by mechanical strength. A heat-transfer calculation using ANSYS suggested that light elements with practical foil thickness provide higher temperature rise of the foil absorber compared with those of heavier element with practical foil thickness. The maximum of temperature rise was evaluated using a He-Ne laser irradiation onto absorber samples. The material dependence of the temperature rise has a similar tendency between the calculations and the experiments. Experimentally sensitivity of IRVB improved from 280 $\mu W/cm^2$ to 110 $\mu W/cm^2$ using titanium with 1 μm thickness compared with conventional platinum with 2.5 μm thickness. Consequently, the signal-to-noise ratio of IRVB could be improved from 2.8 to 9.1.

I. INTRODUCTION

In fusion reactors, radiative cooling using impurity seeding is a common scenario to reduce divertor heat load. In ITER, 50-60% of the heating power should be dispersed as plasma radiation. The requirement of the fraction increases to 80% In JA-DEMO [1]. Linear devices, e.g., GAMMA10/PDX [2, 3], have important roles to investigate the mechanism of the detachment, e.g., energy balance, and to improve simulation codes. For the study, not only spectroscopic measurement but also plasma radiation measurement is essential. Resistive bolometers are commonly used for plasma radiation measurement mainly in large devices [4]. However, it is too costly, especially for radiation profile measurement with a number of channels. On the other hand, InfraRed imaging Video Bolometer (IRVB) can realize a multi-dimensional measurement using only a foil absorber and an infrared (IR) camera [5-9]. Preliminary results of an IRVB on GAMMA10/PDX suggested that the sensitivity of the IRVB should be improved to realize the sensitivity comparable to that of the measurement on the Large Helical Device, LHD. For the foil absorber, platinum is conventionally used to detect plasma radiation with high energy from the core plasmas [10]. However, the material of the absorber has not been investigated for the plasma radiation with low energy only from divertor plasmas. Therefore, in this paper, sensitivity of the IRVB was improved by focusing on the divertor plasma measurement. In GAMMA10/PDX, the targeted ion temperature is 20 - 500 eV and the targeted electron temperature is 100 eV in the E-divertor region [2, 3]. The ion temperature in the central cell is up to 10 keV [3]. By considering the IRVB has been installed at the upstream region of the E-divertor region, plasma radiation with the photon energy up to 1 keV is considered. The schematic and the sensitivity of the IRVB are shown in Section II. The foil absorber thickness appropriate for the low energy radiation is investigated in various materials in Section III. The

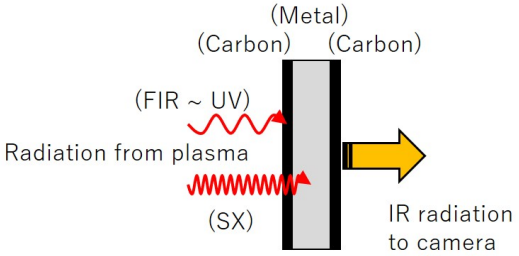

FIG. 1. (Color online). Schematic of a foil absorber of IRVB.

[a)]Author to whom correspondence should be addressed: mukai.kiyofumi@nifs.ac.jp.

temperature rise of the foil absorber is evaluated by using a heat-transfer calculation and using He-Ne laser irradiation experiments onto absorber samples in Section IV.

II. INFRARED IMAGING VIDEO BOLOMETER

A. Schematic of IRVB

The IRVB consists of a pinhole camera and an IR camera. Plasma radiation through an aperture is projected onto a foil absorber inside a vacuum vessel. The two-dimensional temperature distribution due to plasma radiation is observed using an IR camera. A foil absorber has three layers as shown in FIG. 1. Both sides of a thin metal foil are blackened by carbon. Radiations in the range of far infrared, visible, and ultraviolet are absorbed in the carbon layer on the plasma side. Radiations in the range of soft X-ray is absorbed in the metal layer. The carbon layer on the IR camera side can increase emissivity to improve sensitivity.

B. SENSITIVITY of IRVB

This equation indicates the sensitivity of the IRVB measurement as Noise Equivalent Power Difference (NEPD, σ_{IRVB}.

$$\sigma_{IRVB} = \frac{\sqrt{10}kt_f\sigma_{IR}}{\sqrt{f_{IR}N_{IR}}}\sqrt{\frac{N_{bol}^3 f_{bol}}{A_f^2} + \frac{N_{bol}f_{bol}^3}{5\kappa^2}}, \quad (1)$$

Here, k, κ, and t_f are the thermal conductivity, the thermal diffusivity, and the thickness of the foil absorber, respectively. A_f is the utilized area of the absorber. σ_{IR} and f_{IR} are the noise equivalent temperature difference and frame rate of an IR camera, respectively. N_{IR} is the number of available pixels of the IR camera which observes the absorber. f_{bol} is frame rate of the IRVB. N_{bol} is the number of bolometer pixels, i.e., the number of detectors into which the foil absorber is divided.

An IRVB has been installed on GAMMA10/PDX. The IR camera is FLIR/ Tau 2 336 (336 pixel × 256 pixel, noise equivalent temperature difference < 50 mK, frame rate = 60 Hz). The foil absorber coated by graphite on both sides is consisted of Pt with 2.5 μm thickness, which is same as the absorber in LHD. As the result of preliminary measurement in GAMMA10/PDX, temperature rise on the foil absorber was up to 1/5 of LHD. In LHD [11], σ_{IRVB} is 1200 μW/cm^2 without time averaging and signal-to-noise ratio, SNR_{bolo} in TABLE II of [12], is 3.4. In GAMMA10/PDX, while σ_{IRVB} in the preliminary setting is 280 μW/cm^2, the SNR_{bolo} remains 2.8 using 1/5 P_{IRdet} [12] of LHD. Therefore, further σ_{IRVB} improvement is required in GAMMA10/PDX to realize the comparable SNR_{bolo} to that in LHD for the measurement even in lower radiation plasmas using various impurity gases for the plasma detachment.

Sensitivity improvement of an IRVB is equivalent to a decrease of σ_{IRVB}. From the viewpoint of the foil absorber, the product of k and t_f should be decreased. σ_{IRVB} can also decrease with the increase of κ. However, κ is proportional to k $\left(\kappa = k/\left(\rho c_p\right)\right)$. Therefore, the decrease of κ is

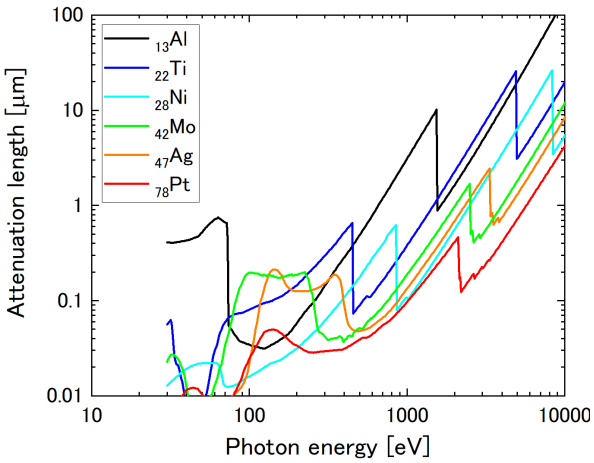

FIG. 2. (Color online). Relation between the photon energy and the attenuation length in various materials.

TABLE I. Material dependence of absorber thickness to detect the radiation with photon energies up to 1 keV, $t_f^{1\ keV}$, and "practical" minimum thickness, t_f^{min}, considering the mechanical strength.

Material	$t_f^{1\ keV}$ [μm]	t_f^{min} [μm]
$_{13}$Al	3.0	3
$_{22}$Ti	0.7	1
$_{23}$V	0.6	1
$_{24}$Cr	0.5	1
$_{25}$Mn	0.6	1
$_{26}$Fe	0.6	1
$_{27}$Co	0.6	1
$_{28}$Ni	0.7	1
$_{29}$Cu	0.8	1
$_{30}$Zn	0.9	1
$_{40}$Zr	0.4	1
$_{41}$Nb	0.3	1
$_{42}$Mo	0.2	1
$_{45}$Rh	0.2	6
$_{46}$Pd	0.2	0.5
$_{47}$Ag	0.2	1
$_{48}$Cd	0.3	1
$_{49}$In	0.4	2
$_{50}$Sn	0.4	3
$_{72}$Hf	0.3	4
$_{73}$Ta	0.16	5
$_{74}$W	0.13	5
$_{75}$Re	0.2	12.5
$_{77}$Ir	0.1	10
$_{78}$Pt	0.1	2.5
$_{79}$Au	0.1	2

basically incompatible with the decrease of kt_f. Here, ρ and c_p are density and specific heat capacity, respectively. Basically, reduction of kt_f by changing the material of the metal layer of the absorber is the most effective way to reduce σ_{IRVB}.

σ_{IRVB} can be decreased also from the viewpoint of IR camera and its field of view [12-14]. However, in this paper, sensitivity improvement was considered by focusing on the foil absorber material.

III. MATERIAL DEPENDENCE of FOIL ABSORBER THICKNESS

If a thinner foil is used, a higher sensitivity can be obtained as mentioned above. On the other hand, in order to absorb the photon with a certain energy, the foil absorber needs a thickness which is determined by the attenuation length of photons in the material. The material dependence of foil absorber thickness was investigated for the measurement including high-energy radiation from core plasmas [10]. According to the comparison among Ta, W, Pt, and Au, Pt with 2.5 μm thickness was optimal. The relation between the photon energy and the attenuation length in various materials [15] is shown in FIG. 2. Drastic changes of the attenuation length are due to absorption end. The absorber thickness for the measurement with lower photon energy up to 1 keV was estimated as $t_f^{1\,keV}$ by the relation. Material dependence of $t_f^{1\,keV}$ is shown in TABLE 1. In the case of Pt, 0.1 μm is sufficient for the absorber thickness. However, such a thin foil is easy to tear. Therefore, by considering the mechanical strength, a "practical" minimum thickness was evaluated as t_f^{min}. The criterion was that foil with the size of 50 mm × 50 mm or larger is commercially available without support like an acrylic plate. Material dependence of t_f^{min} is also shown in TABLE 1. $t_f^{1\,keV}$ decreases with the increase of the atomic number. On the other hand, due to the mechanical strength, t_f^{min} tends to increase with the increase of atomic number.

IV. MATERIAL DEPENDENCE of TEMPERATURE RISE on FOIL ABSORBER

A. TEMPERATURE RISE EVALUATION USING HEAT-TRANSFER CALCULATION

A steady-state heat-transfer calculation was performed to investigate the material dependence of the temperature rise. The maximum temperature rise, ΔT_{max}, due to a certain heat flux was evaluated using ANSYS. The calculation model was a simple cylinder with a diameter of 37 mm. The cylinder consisted of three layers: carbon, metal, and carbon. The thickness of the metal layer was t_f^{min} as shown in TABLE I. The thickness of the carbon layers was assumed 5 μm which was evaluated in a previous study [16]. The boundary temperature on the edge of the cylinder was fixed at 300 K. Gaussian heat flux was applied at the center on the carbon layer of plasma side. The heat flux simulated He-Ne laser irradiation as described below. Blackbody radiation from the surface of the carbon layers was applied with the assumption that the emissivity is 1. The

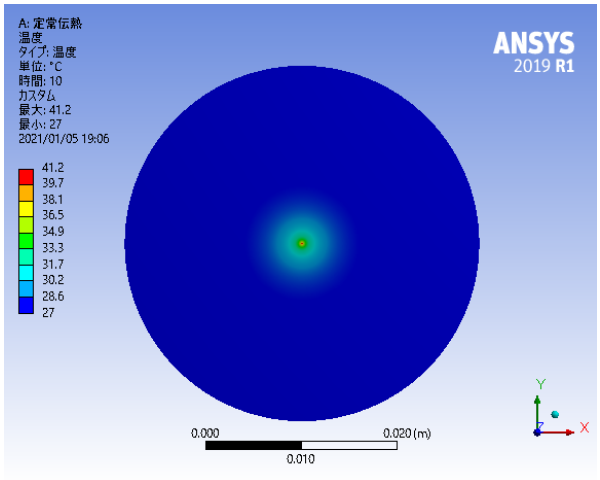

FIG. 3. (Color online). Two-dimensional temperature profile simulated by the heat-transfer calculation, ANSYS.

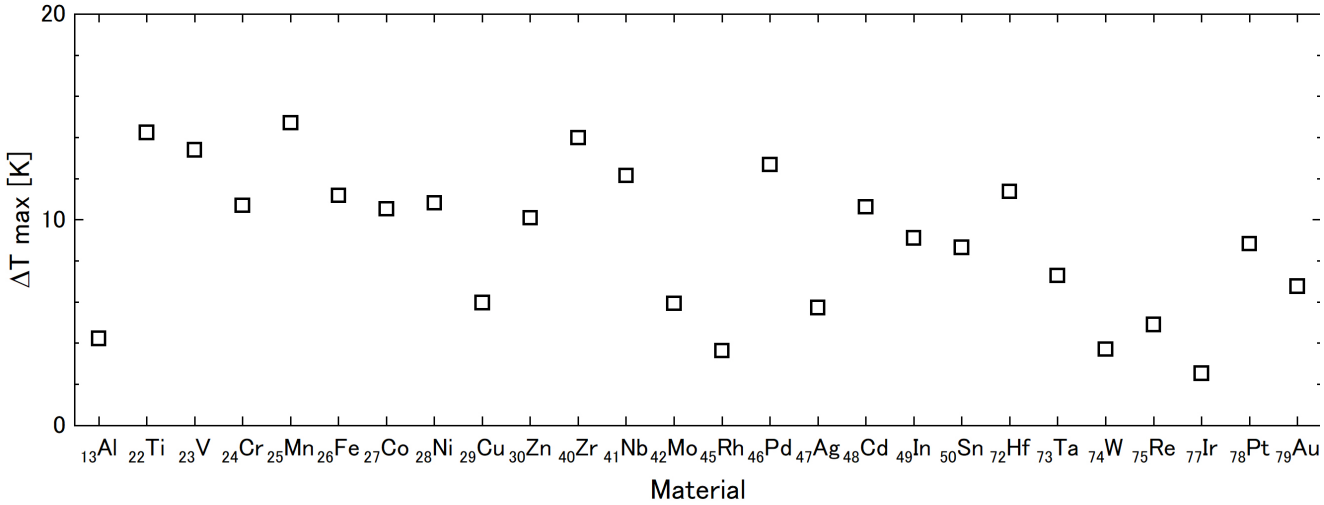

FIG. 4. Material dependence of ΔT_{max} evaluated using heat-transfer calculation. The thickness of the metal layer was t_f^{min} as shown in TABLE I.

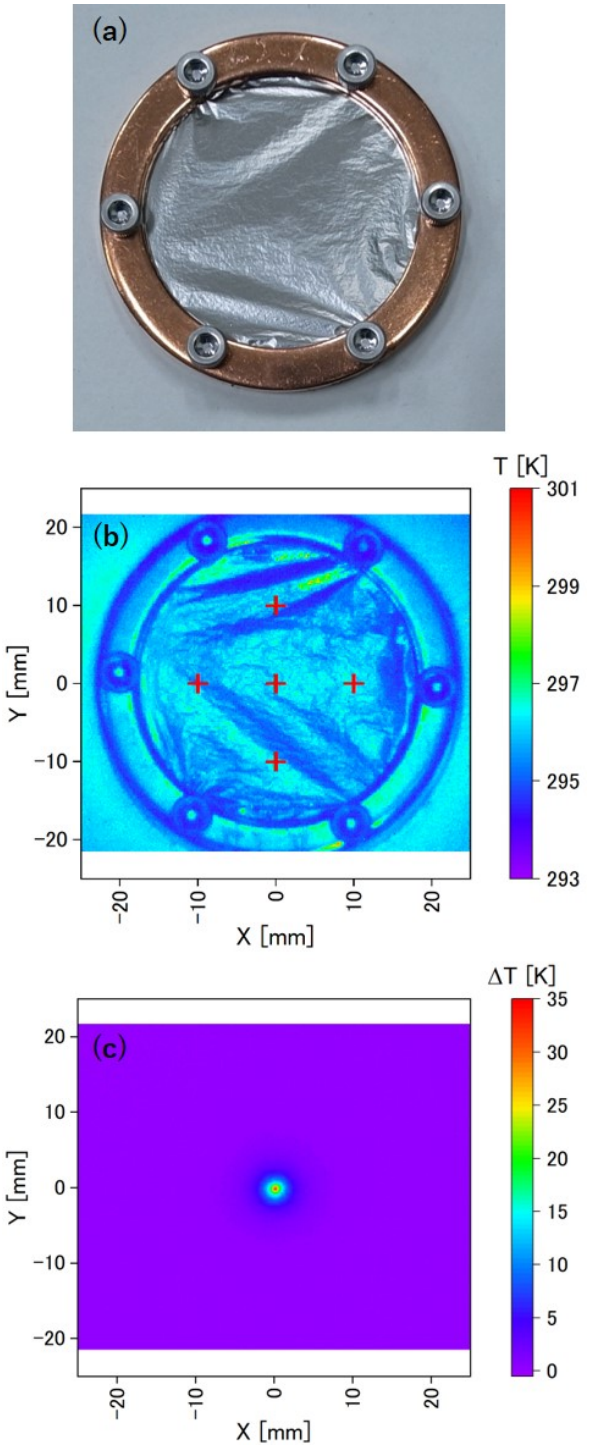

FIG. 5. (Color online). (a) Sample of foil absorber before carbon coating. (b) IR image of the sample without laser irradiation. "+" indicate the irradiation points. (c) Temperature rise, ΔT, profile due to the laser irradiation.

environmental temperature for blackbody radiation was also fixed at 300 K.

A temperature profile simulated by the heat-transfer calculation is shown in FIG. 3. The material dependence of ΔT_{max} is shown in FIG. 4. ΔT_{max} tends to increase above that of conventional Pt with the decrease of atomic number while Al had lower ΔT_{max} due to its higher t_f^{min}. Mn had the highest ΔT_{max}. However, since Mn is a magnetic substance, Mn is not appropriate to use for the measurement on magnetically confined plasma devices. Therefore, Ti is considered the best material which had the second highest ΔT_{max}.

B. TEMPERATURE RISE EVALUATION USING HE-NE LASER IRRADIATION EXPERIMENT

ΔT_{max} in steady-state was evaluated also experimentally using a He-Ne laser irradiation. FIG. 5 (a) shows a foil absorber sample before carbon coating. A metal foil was held by two oxygen-free copper ring frames with inner diameters of 37 mm. Al, Ti, Ni, Mo, Ag, and Pt were used for the samples with the thickness of t_f^{min} as shown in TABLE I. Both sides of the foil are coated by graphite spray (Henkel AG & Co. KGaA/ BONDERITE S-AD AERODAG G AN). A He-Ne laser with the wavelength of 632.8 nm is irradiated onto the foil sample in vacuum. The $1/e^2$ width was 0.2 mm and the power was 5.8 mW. The temperature profile is observed from the backside using an IR camera (FLIR/ A655sc). ΔT_{max} was evaluated as the average of the irradiations to five points (center and the 10 mm away in four directions) as shown in FIG. 5 (b). ΔT profile due to the laser irradiation is shown in FIG. 5 (c). Influence of the foil wrinkles could be subtracted as a background.

FIG. 6 shows the material dependence of ΔT_{max} as a comparison between the laser irradiation experiment and the heat-transfer calculation. ΔT_{max} of Ti with 1 μm thickness doubled that of Pt with 2.5 μm thickness. The tendency of the material dependence of ΔT_{max} is similar between the experiment and the calculation. One of the reasons for the difference between the experiment and the calculation can be considered as the error in the thickness of the metal and carbon layers. Cross-section observation using a scanning

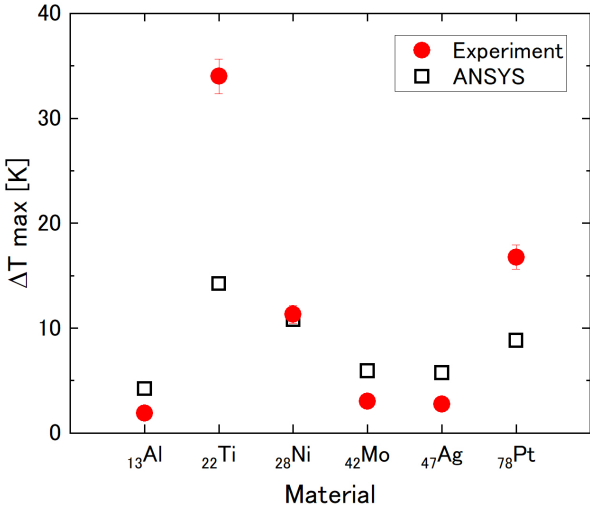

FIG. 6. (Color online). Material dependence of ΔT_{max} as a comparison between the laser irradiation experiment and the heat-transfer calculation from ANSYS. The thickness of the metal layer was t_f^{min} as shown in TABLE I.

electron microscope and/or a transmission electron microscope is required for detailed analysis. A possible reason for the difference of experimental values of k from its literature values is the plastic deformation in the foil caused by the rolling method used in the manufacturing process.

σ_{IRVB} estimated using typical thermal characteristics of Ti and using current IR camera settings in GAMMA10/PDX is 90 μW/cm^2. Consequently, SNR_{bolo} is improved from 2.8 to 9.1. Here, it should be noted that σ_{IRVB} and SNR_{bolo} do not change significantly when k is halved. Since k is proportional to κ and the term related to κ is dominant in the root term of Eq. (1), the halved k is countered by $\sqrt{1/\kappa^2}$.

V. SUMMARY

Sensitivity of the IRVB was improved for measurement of relatively low energy plasma radiation from the viewpoint of a metal foil absorber material. The photon energy of the radiation was considered up to 1 keV for divertor plasma measurement. The thickness of a foil absorber was evaluated not only for conventional heavy elements, e.g., Pt, but also for light elements by the relation between photon energy and attenuation length and by mechanical strength. A heat-transfer calculation using ANSYS suggested that light elements with practical foil thickness provide higher temperature rise compared with those of heavy elements with practical foil thickness. The maximum of temperature rise was evaluated using a He-Ne laser irradiation onto absorber samples. Material dependence of the temperature rise has a similar tendency between the calculations and the experiments. Sensitivity of IRVB could improve from 280 μW/cm^2 to 90 μW/cm^2 using Ti with 1 μm thickness instead of conventional Pt with 2.5 μm thickness. Consequently, SNR_{bolo} could be improved from 2.8 to 9.1.

In this paper, a graphite spray was used for the blackening of the foil absorber. However, heat-transfer calculation suggested that a thinner carbon coating can improve the sensitivity further. A vapor deposition technique is a candidate for the further sensitivity improvement. The improved foil absorber will be applied to plasma radiation measurements not only on GAMMA10/PDX but also on a medium-sized helical-axis heliotron device, Heliotron J. The foil absorber with high sensitivity is available for divertor plasma measurements also in the large devices. IRVBs can increase the channels by finely dividing the foil absorber in analysis. Therefore, the higher-sensitivity foil absorber can provide higher spatial resolution measurement with the same signal to noise ratio.

ACKNOWLEDGMENTS

This work was supported by JSPS KAKENHI Grant No. JP17K14900, JP19K14689, by NIFS/NINS Grant No. NIFS18ULHH038, NIFS14KUGM086, IFS19KUHL089, and by grant of Future Energy Research Association.

Data availability: The data that support the findings of this study are available from the corresponding author upon reasonable request.

REFERENCES

[1]N. Asakura, K. Hoshino, H. Utoh, Y. Someya, S. Suzuki, C. Bachmann, H. Reimerdes, R. Wenninger, H. Kudo, S. Tokunaga *et al*., Fusion Eng. Des. **136**, 1214 (2018).
[2]M. Sakamoto, K. Oki, Y. Nakashima, Y. Akabane, Y. Nagatsuka, M. Yoshikawa, R. Nohara, K. Hosoi, H. Takeda, K. Ichimura *et al*., Trans. Fusion Sci. Technol. **63**, 188 (2013).
[3]Y. Nakashima, K. Ichimura, M. S. Islam, M. Sakamoto, N. Ezumi, M. Hirata, M. Ichimura, R. Ikezoe, T. Imai, T. Kariya *et al*., Nucl. Fusion **57**, 116033 (2017).
[4]K. F. Mast, J. C. Vallet, C. Andelfinger, P. Betzler, H. Kraus, and G. Schramm, Rev. Sci. Instrum. **62**, 744 (1991).
[5]B. J. Peterson, Rev. Sci. Instrum. **71**, 3696 (2000).
[6]B. J. Peterson, H. Parchamy, N. Ashikawa, H. Kawashima, S. Konoshima, A. Y. Kostryukov, I. V. Miroshnikov, D. C. Seo, and T. Omori, Rev. Sci. Instrum. **79**, 10E301 (2008).
[7]K. Mukai, S. Masuzaki, B. J. Peterson, T. Akiyama, M. Kobayashi, C. Suzuki, H. Tanaka, S. N. Pandya, R. Sano, G. Motojima *et al*., Nucl. Fusion **55**, 083016 (2017).
[8]K. Mukai, B. J. Peterson, S. Takayama, and R. Sano, Rev. Sci. Instrum. **87**, 11E124 (2016).
[9]K. Mukai, R. Abe, B. J. Peterson, and S. Takayama, Rev. Sci. Instrum. **89**, 10E114 (2018).
[10]R. Sano, B. J. Peterson, E. A. Drapiko, Y. Watanabe, Y. Yamauchi, and T. Hino, Plasma Fusion Res. **6**, 2406076 (2011).
[11]K. Mukai, T. Nishitani, K. Ogawa, and B. J. Peterson, IEEE Transactions on Plasma Science **47** (1), 18 (2019).
[12]S. N. Pandya, B. J. Peterson, K. Mukai, R. Sano, A. Enokuchi, and N. Takeyama, Rev. Sci. Instrum. **85**, 073107 (2014).
[13]B. J. Peterson, S. Konoshima, A. Y. Kostryukov, D. C. Seo, Y. Liu, I. V. Miroshnikov, N. Ashikawa, H. Parchamy, H. Kawashima, N. Iwama *et al*., Plasma Fusion Res. **2**, S1018 (2007).
[14]K. Mukai, B. J. Peterson, S. N. Pandya, R. Sano, and M. Itomi, Plasma Fusion Res. **9**, 3402037 (2014).
[15]The Center for X-Ray Optics, Lawrence Berkeley National Laboratory, *X-Ray Attenuation Length*, http://henke.lbl.gov/optical_constants/atten2.html
[16]S. N. Pandya, B. J. Peterson, R. Sano, K. Mukai, E. A. Drapiko, A. G. Alekseyev, T. Akiyama, M. Itomi, and T. Watanabe, Rev. Sci. Instrum. **85**, 054902 (2014).